Available online at www.sciencedirect.com
SCIENCE DIRECT®
Journal of Catalysis 222 (2004) 100–106
JOURNAL OF CATALYSIS
www.elsevier.com/locate/jcat

SCR of NO_x by C_3H_6: comparison between $Cu/Cr/CeO_2$ and $Cu/Ag/CeO_2$ catalysts

N.A.S. Amin,* E.F. Tan, and Z.A. Manan

Chemical Engineering Department, Faculty of Chemical and Natural Resources Engineering, Universiti Teknologi Malaysia, 81310 Skudai, Johor, Malaysia

Received 4 July 2003; revised 17 September 2003; accepted 8 October 2003

Abstract

The influence of cocations (Cr and Ag) on the activity of Cu/CeO_2 catalysts in the selective reduction of NO_x with C_3H_6 has been investigated in this study. The reduction of NO_x under lean conditions was greatly improved by loading Cr and Ag onto a Cu/CeO_2 catalytic system. All the synthesized bimetal catalysts were characterized using XRD and TPR-H_2. The better metal–support interaction and metal dispersion shown by $Cu/Ag/CeO_2$ have elevated its performance compared to the $Cu/Cr/CeO_2$ catalyst. By having such salient features, the competitiveness factor ($S_{SCR\text{-}HC}$) assigned by $Cu/Ag/CeO_2$ was generally better than that of the other tested catalysts. The presence of O_2 was proven to be a very crucial factor for promoting the selective reduction of NO_x with C_3H_6.

Keywords: Selective reduction of NO_x with C_3H_6; CeO_2; Cu; Cr; Ag

1. Introduction

The selective catalytic reduction of NO_x with hydrocarbons (SCR-HC) has attracted much attention, because it has the potential ability to eliminate NO_x emission from the oxygen-rich exhaust. Cu is identified as one of the most promising elements reported to be active in the SCR-HC [1–3]. Various kinds of metal oxide-supported Cu catalysts have been thoroughly investigated in the SCR-HC such as Cu/SiO_2 [3,4], Cu/Al_2O_3 [5–7] and Cu/ZrO_2 [8,9].

The cerium oxide (CeO_2), which was demonstrated to be capable of reducing SO_x and soot, was deliberated as a possible catalyst support to enhance NO_x removal [10,11]. Muraki et al. [12] discovered that the platinum-modified CeO_2 catalysts were able to reduce NO_x in a wide range of temperatures under lean conditions. Further, it is reported that the Cu/CeO_2 catalyst was capable of eliminating NO_x below 623 K when *n*-butane was used as reductant [13]. However, most of the previous studies on Cu/CeO_2 catalysts were focused on the NO + CO reaction [14–16] and the oxidation of CO by O_2 [17,18]. Therefore, this study could provide a better understanding of the role played by Cu/CeO_2 in the SCR-HC.

The bimetal catalyst concept was introduced in the SCR-HC to improve the performance of the supported Cu catalyst by adding certain promoters [19–22]. The cocation-promoted copper catalysts have been extensively zeolite-based catalytic systems in NO_x abatement [23–26]. The addition of transition metal cocations (Fe, Co, Ni, V, Mn, W, Mo, and Cr) onto zeolite-supported copper catalyst has been reported to tremendously increase the conversion of NO_x under lean conditions [19]. Although these multifunctional catalysts were introduced, the deactivation of the catalysts by dealumination and weak SO_2 resistance are the major obstacles that hinder the application of zeolite-based catalysts in real applications [27]. As a result, the metal oxide-supported copper catalyst is deliberated as a potential exemplary candidate for SCR-HC. Various kinds of reactions have been examined over a supported Cu–Cr system such as the oxidation of CO [28–30], NO + CO reaction [31–33], and NO decomposition [34]. For the NO + CO reaction, the catalytic performance of copper-supported catalyst was significantly affected by the addition of Cr. The Cu–Cr system exhibited an overall better performance than the single metal catalytic system (Cu, Co, and Ni) and three-way catalytic converter [32,33]. All the literature discussed above unambiguously show that there is very little effort devoted to investigation of the application of the Cu–Cr catalytic system in the SCR-HC.

* Corresponding author.
E-mail address: r-naishah@utm.my (N.A.S. Amin).

0021-9517/$ – see front matter
doi:10.1016/j.jcat.2003.10.005

Apart from that, a review of early work also stated that relatively little literature is available on the application of the supported Cu–Ag catalyst in the SCR-HC. Despite Cr, silver was chosen as a cocation for Cu/CeO_2 in this investigation based on various reasons: it possesses a relatively low affinity for water [27], is active by itself [35,36], and produces less N_2O [37]. This paper compares the activity of $Cu/Ag/CeO_2$ with Cu/CeO_2 and $Cu/Cr/CeO_2$ in the selective reduction of NO_x with C_3H_6. The results on the performance of Cu/CeO_2 and $Cu/Cr/CeO_2$ in SCR-HC have recently been reported [38]. In that paper it was unequivocally reported that $Cu/Cr/CeO_2$ with 4 and 3 wt% of Cu and Cr, respectively, showed the best performance for SCR-HC. The influences of reaction temperature and time factor on the performance of the best catalyst in SCR-HC determined in this work have also been examined. All the catalysts were thoroughly characterized using X-ray diffraction (XRD) and temperature-programmed reduction by H_2 (TPR-H_2).

2. Experimental

2.1. Catalyst preparation

CeO_2 powder (Merck) was used as the catalyst support. The BET surface area of the CeO_2 was 3.6 m^2/g. The Cu/CeO_2 catalyst with 4 wt% of Cu and the Ag/CeO_2 with 3 wt% of Ag were synthesized by impregnating the CeO_2 powder with a known quantity of aqueous solution of copper nitrate or silver nitrate (molarity = 1 M), respectively. The solutions were stirred constantly for 17 h at room temperature. Then, the samples were filtered and dried overnight in an oven at 383 K. Finally, the dried catalysts were calcined at 823 K in a box furnace for 5 h.

The coimpregnation method was employed to synthesize the $Cu/Cr/CeO_2$ and $Cu/Ag/CeO_2$ catalysts. In this case, the $Cu/Cr/CeO_2$ catalyst with 4 wt% of Cu and 3 wt% of Cr was prepared by impregnating CeO_2 powder with a copper nitrate aqueous solution and a chromium nitrate aqueous solution (molarity = 1 M) simultaneously. Subsequently, the solution was stirred constantly for 17 h at room temperature. Then, the sample was filtered and dried overnight in an oven at 383 K. Finally, the dried catalyst was calcined at 823 K in a box furnace for 5 h. All the procedures in preparing the $Cu/Cr/CeO_2$ catalyst were repeated to produce the $Cu/Ag/CeO_2$ catalyst except that the 3 wt% of Cr was changed to 3 wt% of Ag using a silver nitrate aqueous solution (molarity = 1 M). Prior to the catalyst characterization and catalytic performance test, all synthesized catalysts were grounded to less than 200 mesh size (74 μm).

2.2. Catalyst characterization

All synthesized catalysts were characterized using XRD and TPR-H_2. XRD patterns were acquired using a Siemen D5000 employing Cu-K_α radiation ($\lambda = 1.54056$ Å). The X-ray tube was operated at 40 kV and 30 mA with 2θ ranging from 5 to 80°. The scanning speed applied in this analysis was 0.05°/s. Crystallite sizes of metal oxide compounds were determined using the Scherrer equation.

TPR-H_2 was performed using a Micromeritics 2900 TPD/TPR equipped with a thermal conductivity detector. For the H_2 reduction analysis, 0.05 g of catalyst was used and treated with 10% of H_2 in Ar at 50 ml/min. The temperature was ramped linearly from ambient temperature to 873 K at 8.75 K/min.

2.3. Catalytic performance test

A lab-scale fixed-bed reactor (stainless steel 316) with i.d. = 10 mm and length = 300 mm was used to investigate the activity of each synthesized catalyst in SCR-HC at an atmospheric pressure and 673 K. One gram of catalyst supported by ceramic wool was loaded into the lab-scale fixed-bed reactor for the catalyst testing. The temperature of the catalyst bed was controlled by a temperature-programmed reactor furnace (Carbolite VST 12/30/200). Prior to the analysis, the catalyst bed was activated in situ by preheating in a helium flow at 673 K for an hour. After the preheating period, a simulated exhaust gas comprising 2000 ppm NO (B.O.C. special gases, 99.5% purity), 2000 ppm C_3H_6 (B.O.C. special gas, 99.0% purity) and 10% O_2 with balance of He was fed into the reactor at $F/W = 10{,}800$ ml/(g_{cat} h). The flow rate of each reactant line was monitored by four flow meters (Brooks Mass Rate 5700). The concentration of NO_x was analyzed using a NO_x emission analyzer (Bacharach NONOXOR II). The CO_x and O_2 levels in the reactor effluent were measured by a CO_x and O_2 emission analyzer (Kane-May KM900). A gas chromatograph (Perkin-Elmer) equipped with a FID detector was utilized to determine the concentration of unreacted C_3H_6. The N_2 concentration was calculated from atomic nitrogen balance and atomic oxygen balance using the inlet and outlet concentrations of NO, CO, CO_2, and O_2. The reaction results were evaluated in terms of NO_x conversion, C_3H_6 conversion, and competitiveness factor ($S_{\text{SCR-HC}}$, %). The $S_{\text{SCR-HC}}$ was defined as the ratio of oxygen atoms supplied from NO to all oxygen atoms reacting with hydrocarbons to form CO and CO_2 [36,38] as in Eq. (1). The $S_{\text{SCR-HC}}$ is equal to 100% if the hydrocarbon is completely oxidized by NO. It decreases upon increase in the HC + O_2 oxidation rate.

$$S_{\text{SCR-HC}}\ (\%) = \frac{2[N_2]}{2[CO] + 3[CO_2]} \times 100\% \quad (C_3H_6 \text{ as a reductant}). \tag{1}$$

$[N_2]$, [CO], and $[CO_2]$ are expressed as molar flow rates. Finally, the effects of reaction temperature (473–773 K) and time factor (8.33×10^{-6} to 11.90×10^{-6} g_{cat} h/ml) were specifically conducted over the best catalyst found in this study.

3. Results and discussion

3.1. X-ray diffraction

The XRD spectra for CeO_2, Cu/CeO_2, $Cu/Cr/CeO_2$, and $Cu/Ag/CeO_2$ catalysts are presented in Fig. 1. It was observed that all synthesized Cu/CeO_2, $Cu/Cr/CeO_2$, and $Cu/Ag/CeO_2$ catalysts exhibited the same pattern of diffraction peaks with the parent CeO_2. No shift was detected in the diffraction lines of the catalysts compared to pure CeO_2, suggesting that Cu^{2+}, Cr^{3+}, and Ag^{+} might not be substituted for Ce^{4+} in CeO_2 [13]. The sizes of XRD-detectable crystallites calculated using the Scherrer equation for all catalysts are tabulated in Table 1 and ranged from 0.078 to 0.124 μm.

Based on the XRD diffractograms, the growth of crystallite phases was detected over all synthesized catalysts. The formation of crystallite phases is due to the high metal loading on the support that has weakened the metal–support interaction [29,39]. As a result, the metal oxides easily interacted with each other and tend to agglomerate to form bulky metal oxide particles at high metal loading [40]. Upon calcining in air, the agglomerated metal oxide particles will form XRD-traceable crystallite phase as depicted in Fig. 1.

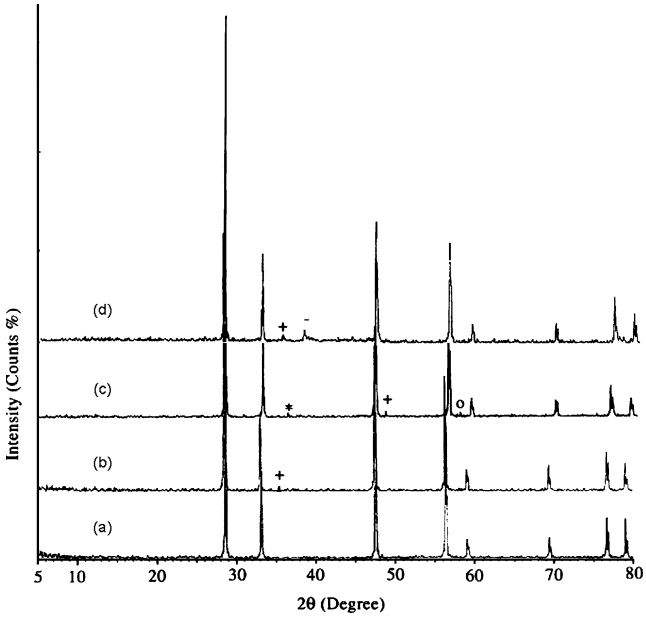

Fig. 1. XRD patterns for CeO_2, Cu/CeO_2, $Cu/Cr/CeO_2$, and $Cu/Ag/CeO_2$. (a) CeO_2; (b) Cu/CeO_2; (c) $Cu/Cr/CeO_2$; (d) $Cu/Ag/CeO_2$. (+) CuO; (*) Cr_2O_3; (○) $CuCr_2O_4$; (−) Ag_2O.

Table 1
Sizes of XRD-detectable crystallites for CeO_2, Cu/CeO_2, $Cu/Cr/CeO_2$, and $Cu/Ag/CeO_2$

Catalyst	Crystallite	Average size (μm)
CeO_2	CeO_2	1.030
Cu/CeO_2	CuO	0.119
$Cu/Cr/CeO_2$	CuO	0.078
	Cr_2O_3	0.124
	$CuCr_2O_4$	0.101
$Cu/Ag/CeO_2$	CuO	0.093
	Ag_2O	0.093

The formation of CuO crystallite was also induced over $Cu/Cr/CeO_2$ and $Cu/Ag/CeO_2$ catalysts due to high metal concentrations. Nevertheless, the size of CuO crystallite formed in the bimetal catalysts was smaller compared to Cu/CeO_2 as presented in Table 1. The reduction in the size of CuO crystallite for bimetal catalysts was generally due to the competitive generation of Cr_2O_3, Ag_2O, and $CuCr_2O_4$, which suppressed the extension growth of CuO crystallites. In the case of $Cu/Cr/CeO_2$, the formation of a $CuCr_2O_4$ spinel was observed and it is expected due to the calcination temperature which was about 773 K [41,42]. In comparison to the $Cu/Cr/CeO_2$, the size of the Ag_2O crystallite in $Cu/Ag/CeO_2$ was generally smaller than those Cr_2O_3 and $CuCr_2O_4$ crystallites. We attribute this to a better metal dispersion and metal-support interaction of small Ag_2O particles on the CeO_2 over the $Cu/Ag/CeO_2$ catalyst. Meanwhile, it seems that the size of CuO crystallite in $Cu/Cr/CeO_2$ was smaller than that in $Cu/Ag/CeO_2$. This was due to the formation of $CuCr_2O_4$ in the $Cu/Cr/CeO_2$ which suppressed the generation of CuO crystallite.

3.2. Temperature-programmed reduction by H_2

The TPR profiles for CeO_2, Cu/CeO_2, $Cu/Cr/CeO_2$, and $Cu/Ag/CeO_2$ catalysts are depicted in Fig. 2. A large peak is observed in the TPR-H_2 profiles of Cu/CeO_2 at 510 K. It was assigned to CuO species as shown in the XRD pat-

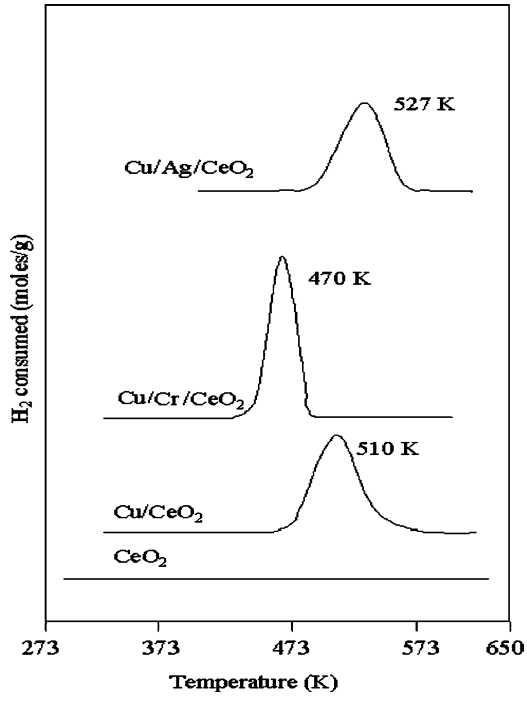

Fig. 2. TPR profiles for the CeO_2, Cu/CeO_2, $Cu/Cr/CeO_2$, and $Cu/Ag/CeO_2$ catalysts.

terns in Fig. 1. In addition, some literature [16,43,44] also stated that the reduction temperature for CuO species ranged from 473 to 523 K. For the $Cu/Cr/CeO_2$ catalyst, a H_2 consumption peak is observed at 470 K as depicted in Fig. 2. In comparison to the XRD patterns (see Fig. 1), the reduction peak should be assigned to CuO, Cr_2O_3, and $CuCr_2O_4$ species. According to Jones and McNicol [45], the combination of CuO species with first-row transition metal ion likes Cr generally produces the same TPR-H_2 profiles as obtained from CuO species except for the reduction peak being shifted to low temperatures as observed in this study. The increase of reduction temperature has been reported to be due to the strong metal–support interaction [43]. In contrast, the decrease of reduction temperature in the TPR-H_2 profiles of $Cu/Cr/CeO_2$ compared to Cu/CeO_2 was attributed to low metal–support interaction caused by metal agglomeration.

For the $Cu/Ag/CeO_2$ catalyst, a large reduction peak centered at 527 K is observed from its TPR profile. Based on the XRD diffractogram (see Fig. 1), the reduction peaks should be assigned to CuO and Ag_2O. The combination of Cu with Ag has also been reported to produce a single peak by Jones and McNicol [45] as observed in this study. The introduction of Ag to the Cu/CeO_2 catalyst has lifted the reduction temperature for the exposed metal active sites to 527 K compared to Cu/CeO_2 (510 K) and $Cu/Cr/CeO_2$ (470 K). Therefore, one can generally expect that the addition of Ag onto Cu/CeO_2 has increased the metal–support interaction and produces active sites which are much more resistant to reduction [40].

3.3. SCR-HC over Cu/CeO_2, $Cu/Cr/CeO_2$, and $Cu/Ag/CeO_2$

Table 2 shows the competitiveness factor ($S_{\text{SCR-HC}}$) and the conversions of NO_x and C_3H_6 achieved over Cu/CeO_2, $Cu/Cr/CeO_2$, and $Cu/Ag/CeO_2$ catalysts. Clearly, the NO_x conversions gained over Cr- and Ag-modified Cu/CeO_2 catalysts were much higher than that of Cu/CeO_2. The $Cu/Ag/CeO_2$ catalyst exhibited the highest NO_x conversion and $S_{\text{SCR-HC}}$. The activities of the catalysts evaluated in terms of NO_x reduction can be arranged in the following order:

$$CeO_2 < Ag/CeO_2 < Cu/CeO_2 < Cu/Cr/CeO_2 < Cu/Ag/CeO_2.$$

It is also interesting to note that the $Cu/Ag/CeO_2$ catalyst exhibited higher NO_x conversion than the $Cu/Cr/CeO_2$, although both catalysts achieved nearly the same C_3H_6 combustion activity. The result implied that the Ag-promoted Cu/CeO_2 catalyst was more selective in reducing NO_x with C_3H_6 than $Cu/Cr/CeO_2$ under lean conditions as indicated by its $S_{\text{SCR-HC}}$ value. However, the favorable effect of the addition of Ag on the catalytic performances of the Cu/CeO_2 catalyst cannot be attributed to Ag itself, which is almost inactive for NO_x reduction at 673 K as shown in Table 2. We attribute this to the coexistence of CuO and Ag_2O species which was believed to grant a promising performance of the $Cu/Ag/CeO_2$ catalyst in SCR-HC.

The comparison between $Cu/Cr/CeO_2$ and $Cu/Ag/CeO_2$ catalysts obviously indicated that the metal–support interaction is a critical factor which determines the performance of the catalyst. Based on the XRD and TPR results, the metal oxides were much more well dispersed and caused better metal–support interaction in the $Cu/Ag/CeO_2$ compared to the $Cu/Cr/CeO_2$ catalyst. Generally, the well-dispersed metal cocations will exhibit better promoting results as reported by the studies over $AgCl/Al_2O_3$ [46], Ag/Al_2O_3 [47], and Co/ZrO_2 [48]. Kung and Kung [4] have also stated that the NO species are more readily adsorbed on the highly dispersed metal oxide species while the agglomerated metal favors the adsorption of O_2 and induces the combustion of hydrocarbon. Moreover, the reaction intermediates produced from hydrocarbon oxidation are different on dispersed versus agglomerated metal species. The reaction intermediates generated on highly dispersed metal oxide species are selective to react with NO than those on agglomerated metal species to form N-containing species, which then react with another NO molecule to form N_2 [4]. Hence, the characterization results unequivocally demonstrate that the well-dispersed metal oxide species on the surface of $Cu/Ag/CeO_2$ has promoted a better reduction of NO_x than $Cu/Cr/CeO_2$ even if both catalysts achieved comparable C_3H_6 consumption activities.

Table 2
Catalytic performance of the CeO_2, Ag/CeO_2, Cu/CeO_2, $Cu/Cr/CeO_2$, and $Cu/Ag/CeO_2$ catalysts evaluated in terms of N_2 selectivity, $S_{\text{SCR-HC}}$, NO_x, and C_3H_6 conversions at 1 atm and 673 K

	Conversion (%)		N_2 selectivity[a]	$S_{\text{SCR-HC}}$
	NO_x	C_3H_6	(%)	(%)
CeO_2	25.1	100	100	0.7
Ag/CeO_2	31.5	45.4	100	3.5
Cu/CeO_2	40.2	100	100	4.2
$Cu/Cr/CeO_2$	80.7	62.0	100	15.2
$Cu/Ag/CeO_2$	87.1	61.6	100	16.3

(Reaction conditions: 2000 ppm NO, 2000 ppm C_3H_6, 10% O_2 with balance of He, $F/W = 10{,}800$ ml/(g_{cat} h)).

[a] N_2 selectivity $= 2 \times 100\% \times [N_{2,\text{formed}}]/[NO_{\text{inlet}} - NO_{\text{outlet}}]$.

3.4. Catalytic performance of $Cu/Ag/CeO_2$

The $Cu/Ag/CeO_2$ was deliberated as the most promising bimetal catalyst to be effective in the selective reduction of NO_x with C_3H_6 under lean conditions in this study. Extended investigations were carried out using the $Cu/Ag/CeO_2$ catalyst over a wide range of time factors (8.33×10^{-6} to 11.90×10^{-6} g_{cat} h/ml) and temperature (473–773 K) in order to gains a deeper insight into the applicability of the catalyst under more realistic conditions. In Fig. 3, the conversions of C_3H_6 and NO_x achieved over a $Cu/Ag/CeO_2$ catalyst at various time factors and reaction temperatures are presented. The temperature at which

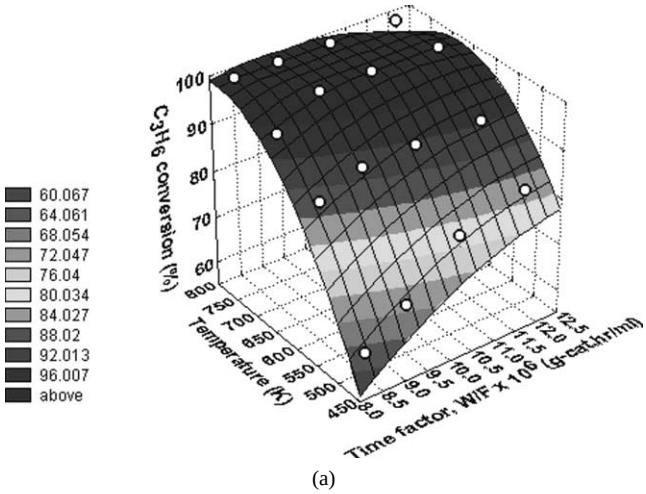

(a)

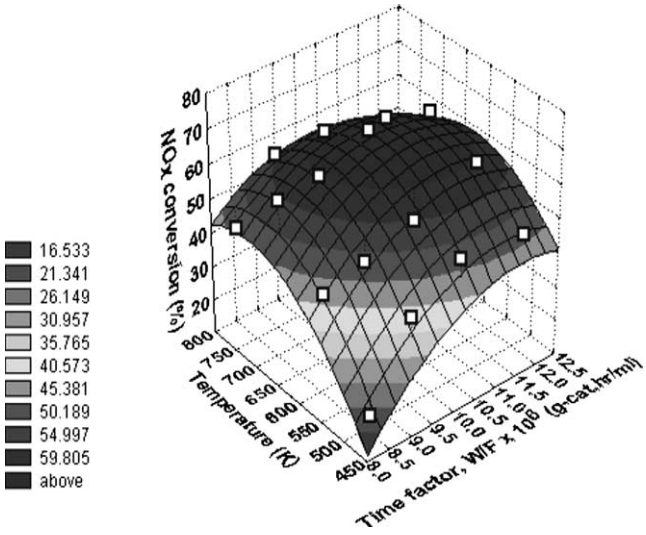

(b)

Fig. 3. Effects of reaction temperature and time factor, W/F on (a) C_3H_6 and (b) NO_x conversions for $Cu/Ag/CeO_2$ (reaction mixture: 2000 ppm NO, 2000 ppm C_3H_6, 10% O_2 with balance of He).

the NO_x conversion reached its maximum (673 K) corresponds to the temperature where nearly maximum oxidation of the C_3H_6 was achieved as observed in Cu/ZSM-5 [49,50], Cu/Al_2O_3 [2,5,51], and $Ag/\gamma\text{-}Al_2O_3$ [35]. Beyond this optimum temperature (673 K), the NO_x conversion dropped abruptly, regardless of the time factor applied due to the rapid oxidation of C_3H_6 by O_2 [52,53]. The conversion of NO_x has substantially increased upon increasing the time factor from 8.33×10^{-6} to 10.42×10^{-6} g_{cat} h/ml over all temperature ranges. Then, a further increase in the time factor hastily reduced the NO_x conversion. The reduction in NO_x removal at the higher time factor or lower reactant flow rate was mainly caused by the combustion of C_3H_6 [54]. The optimum reaction temperature and time factor for NO_x conversion using the $Cu/Ag/CeO_2$ catalyst are 673 K and 10.42×10^{-6} g_{cat} h/ml, respectively.

In Fig. 4, the competitiveness factor ($S_{SCR\text{-}HC}$) determined over the $Cu/Ag/CeO_2$ catalyst at various temperatures and time factors is shown. At a low reaction temperature range (473–573 K), the maximum $S_{SCR\text{-}HC}$ value was obtained at a time factor around 10×10^{-6} g_{cat} h/ml. Then, the $S_{SCR\text{-}HC}$ was decreased as the time factor was increased. The results indicated that the oxidation of C_3H_6 by O_2 was favored over the NO + C_3H_6 reaction at a high time factor and hindered the reduction of NO_x as shown in Fig. 3. The maximum value of $S_{SCR\text{-}HC}$ was shifted to low time factor (8.33×10^{-6} g_{cat} h/ml) as the study was conducted at 673 and 773 K. At a high reaction temperature range (673–773 K), the $S_{SCR\text{-}HC}$ value was definitely reduced when the time factor was adjusted from 9.26×10^{-6} to 11.90×10^{-6} g_{cat} h/ml. The decline in the $S_{SCR\text{-}HC}$ value could be attributed to the C_3H_6 oxidation by O_2 that became a dominant reaction and obstructed the reduction of NO_x with C_3H_6 as the time factor is increased. The experiment conducted at 773 K exhibited the lowest $S_{SCR\text{-}HC}$ value compared to others. The $S_{SCR\text{-}HC}$ is rather low at the high temperature range because hydrocarbon oxidation by O_2 prevails over hydrocarbon oxidation by NO [3,55].

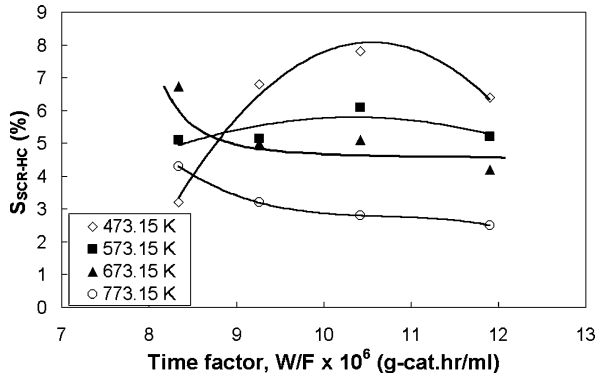

Fig. 4. Influences of reaction temperature and time factor, W/F on $S_{SCR\text{-}HC}$ for $Cu/Ag/CeO_2$ (reaction mixture: 2000 ppm NO, 2000 ppm C_3H_6, 10% O_2 with balance of He).

The selective reduction of NO_x with C_3H_6 examined over $Cu/Ag/CeO_2$ catalysts did not yield any nitrous oxide (N_2O) since the N_2 selectivity was 100% as shown in Table 2. The reacted NO was fully converted into N_2. A similar observation has also been reported over Cu/Ag/ZSM-5 [27] that employed comparable reaction conditions (2000 ppm NO, 2000 ppm hydrocarbon, 10% O_2 with balance of He, total flow 10 l/h, reaction temperature: 473–873 K) as in this study. Therefore, it is believed that the reaction conditions might have played an important role in eliminating the formation of nitrous oxide (N_2O). The presence of an Ag_2O phase in the $Cu/Ag/CeO_2$ (see Fig. 1) may also be a key factor that attributes to the extinction of N_2O species. The N_2O species formed during the reduction of NO_x are directly decomposed to N_2 over Ag_2O active sites as shown in Eq. (2) [37]:

$$Ag_2O + N_2O \rightarrow 2AgO + N_2. \quad (2)$$

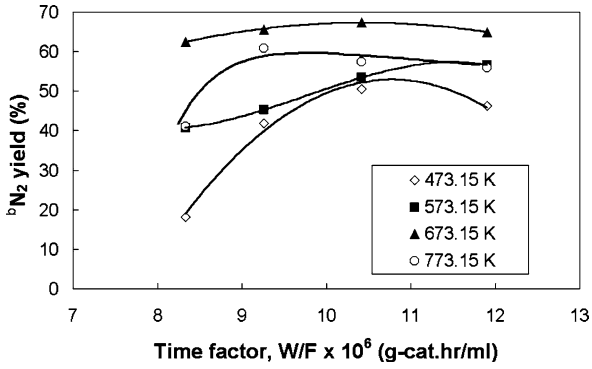

Fig. 5. Effects of reaction temperature and time factor, W/F on N_2 yield for $Cu/Ag/CeO_2$ (reaction mixture: 2000 ppm NO, 2000 ppm C_3H_6, 10% O_2 with balance of He). $^{b}N_2$ yield $= 2 \times (\text{mol } N_{2,\text{formed}})/(\text{mol } NO_{\text{reacted}})$.

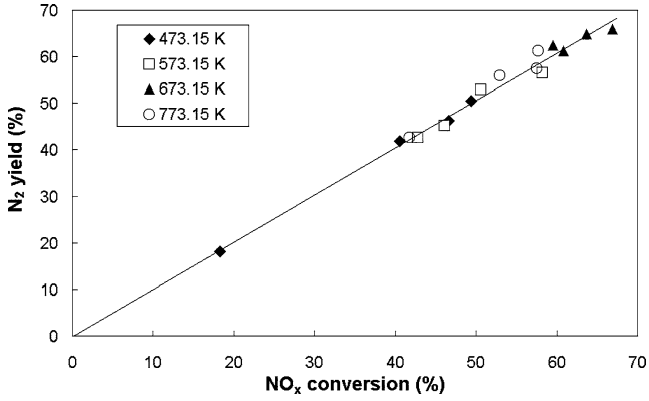

Fig. 6. Effect of the reaction temperature on the relationship of N_2 yield and the conversion of NO_x for the $Cu/Ag/CeO_2$ catalyst (reaction mixture: 2000 ppm NO, 2000 ppm C_3H_6, 10% O_2 with balance of He).

Increasing the amount of Ag_2O was suggested to improve the conversion of NO_x and warrants a high yield of N_2 [37].

Fig. 5 shows the yield of N_2 determined over $Cu/Ag/CeO_2$ catalyst at various reaction temperatures and time factors. The SCR-HC conducted at 673 K provided the highest yield of N_2 over all time factor ranges. Beyond this temperature, the N_2 yield was slightly diminished due to the concomitant oxidation of C_3H_6 by O_2 which impeded the reduction of NO_x by C_3H_6. At a low temperature range (473–573 K), the yield of N_2 obtained over $Cu/Ag/CeO_2$ was much lower than the experiment conducted at 673 K, although its $S_{\text{SCR-HC}}$ value was higher. This was probably due to the reactions not fully activated at a temperature lower than 673 K. The SCR-HC reaction conducted at 473 K showed the lowest yield of N_2 over all time factors studied.

Fig. 6 displays the relationship between the N_2 yield and the conversion of NO_x at various reaction temperatures. All the data are tabulated around a linear curve. Hence, it may be concluded that the reaction temperature employed did not exert a significant effect on the yield of N_2 at a constant conversion level. The yield of N_2 increased as the reaction progressed.

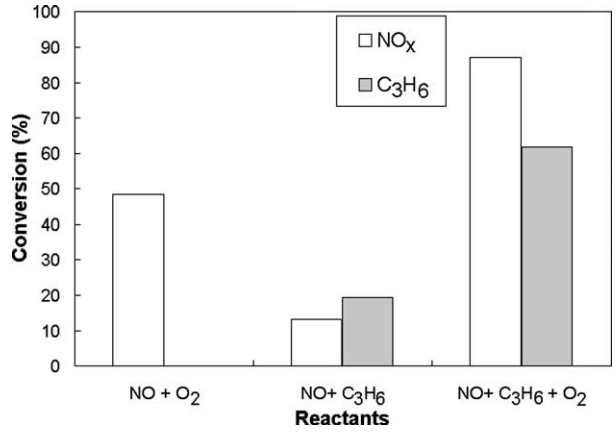

Fig. 7. Effects of oxygen and C_3H_6 on the NO_x conversion investigated over $Cu/Ag/CeO_2$ at 1 atm and 673 K with 10,800 ml/(g_{cat} h).

3.5. Effect of O_2 and C_3H_6 on SCR-HC

Fig. 7 illustrates the conversions of NO_x and C_3H_6 determined over NO + O_2, NO + C_3H_6, and NO + C_3H_6 + O_2 reactions using the $Cu/Ag/CeO_2$ catalytic system. In the absence of O_2, the NO + C_3H_6 reaction did not achieve promising results in terms of NO_x conversion. The direct decomposition of NO_x (NO + O_2) was more favored than the NO + C_3H_6 reaction. According to Hamada et al. [62], silver possesses weak affinity for molecule oxygen. This probably would enhance the NO_x reduction activity and resistance of the catalyst to oxygen poisoning for direct decomposition of NO_x in the presence of oxygen. Among the reactions examined, the presence of C_3H_6 under net oxidizing conditions has greatly promoted the NO_x reduction. By comparing the NO + C_3H_6 + O_2 and NO + C_3H_6 reactions as presented in Fig. 7, the presence of O_2 in the NO-containing stream was proven to be a very essential feature to foster the conversion of NO_x in SCR-HC as found in the literature [56,57].

It has been widely proposed that the roles of O_2 in the NO_x reduction using the SCR-HC method are: (i) to activate NO and hydrocarbons [47,58]; (ii) to maintain a Cu^{+}/Cu^{2+} site balance [50,59]; (iii) to oxidize NO to NO_2 [56,60]; and (iv) to react with carbonaceous deposits [61]. Although no general agreement can be found in the proposed mechanisms involving O_2, Martínez-Arias et al. [47] have elucidated that the formation of oxidized intermediates ($C_xH_yO_z$ for the hydrocarbons and surface NO_x species for NO) originated from the activation of hydrocarbons and NO_x by O_2 generally happens over a catalyst which gains very low selectivity of N_2O or nearly extinct. Consequently, it has been postulated that the reaction mechanism involving O_2 occurring over the $Cu/Ag/CeO_2$ catalyst in this study is the activation of C_3H_6 and NO species by O_2 to form partially oxidized intermediates which later are reduced to N_2.

4. Conclusion

From this study, it is concluded that $Cu/Ag/CeO_2$ showed the best performance in the SCR-HC. In comparison to the $Cu/Cr/CeO_2$ catalyst, the $Cu/Ag/CeO_2$ catalytic system has a better metal oxide dispersion and metal–support interaction. These salient features ultimately promote the NO_x conversion achieved over $Cu/Ag/CeO_2$ in the SCR-HC. Moreover, the presence of O_2 is also very vital for stimulating the selective reduction of NO_x with C_3H_6 using the $Cu/Ag/CeO_2$ catalyst.

Acknowledgments

The authors gratefully acknowledge the financial support received in the form of a research grant (Project No.: 09-02-06-0070) from the Ministry of Science, Technology, and Environment, Malaysia. We also express our special sincere gratitude to the Warwick Process Technology Centre for providing technical support and guidance.

References

[1] M. Iwamoto, H. Yahiro, Catal. Today 22 (1994) 5.
[2] K.-I. Shimizu, H. Maeshima, A. Satsuma, T. Hattori, Appl. Catal. B 18 (1998) 163.
[3] P. Carniti, A. Gervasini, V.H. Modica, N. Ravasio, Appl. Catal. B 28 (2000) 175.
[4] H.H. Kung, M.C. Kung, Catal. Today 30 (1996) 5.
[5] M. Ozawa, H. Toda, O. Kato, S. Suzuki, Appl. Catal. B 8 (1996) 123.
[6] L. Chen, T. Horiuchi, T. Osaki, T. Mori, Appl. Catal. B 23 (1999) 259.
[7] Y. Chi, S.S.C. Chuang, Catal. Today 62 (2000) 303.
[8] H.H. Kung, K.A. Bethke, M.C. Kung, B. Yang, M. Shah, D. Alt, C. Li, Catal. Today 26 (1995) 169.
[9] D. Pietrogiacomi, D. Sannino, S. Tuti, P. Ciambelli, V. Indovina, M. Occhiuzzi, F. Pepe, Appl. Catal. B 21 (1999) 141.
[10] R.J. Farrauto, K.E. Voss, Appl. Catal. B 10 (1996) 29.
[11] A. Trovarelli, C. de Leitenburg, M. Boaro, G. Dolcetti, Catal. Today 50 (1999) 353.
[12] H. Muraki, T. Inoue, K. Oishi, K. Katoh, EP 0,488,250 A1, 1992.
[13] P. Bera, S.T. Aruna, K.C. Patil, M.S. Hedge, J. Catal. 186 (1999) 36.
[14] J. Theis, B. Labarge, SAE Paper 922251, 1992, 77.
[15] P.G. Harrison, I.K. Ball, W. Azelee, W. Daniel, D. Goldfard, Chem. Mater. 12 (2000) 3715.
[16] Y. Hu, L. Dong, J. Wang, W. Ding, Y. Chen, J. Mol. Catal. A Chem. 162 (2000) 307.
[17] A. Martínez-Arias, M. Fernández-García, J. Soria, J.C. Conesa, J. Catal. 182 (1999) 367.
[18] A. Martínez-Arias, M. Fernández-García, O. Gálvez, J.M. Coronado, J.A. Anderson, J.C. Conesa, J. Soria, G. Munuera, J. Catal. 195 (2000) 207.
[19] S. Kasahara, K. Kamiyama, K. Igawa, S. Matsumoto, M. Fukul, T. Suzuki, S. Kondoh, K. Yokota, S. Takeshima, K. Ishibashi, M. Nakano, US Patent 5,270,024, 1993.
[20] M.J. Rokosz, A.V. Kucherov, H.-W. Jen, M. Shelef, Catal. Today 35 (1997) 65.
[21] J.Y. Yan, W.M.H. Sachtler, H.H. Kung, Catal. Today 33 (1997) 279.
[22] Y. Yokomichi, T. Yamabe, T. Kakumoto, O. Okada, H. Ishikawa, Y. Nakamura, H. Kimura, I. Yasuda, Appl. Catal. B 28 (2000) 1.
[23] T. Liese, W. Grünert, J. Catal. 172 (1997) 34.
[24] M.J. Rokosz, A.V. Kucherov, H.-W. Jen, M. Shelef, Catal. Today 35 (1997) 65.
[25] T. Tamura, M. Kumagai, A. Katsuta, US Patent 5,041,272, 1991.
[26] Y. Ukisu, S. Sato, Appl. Catal. B 2 (1993) 147.
[27] Z. Chajar, P. Denton, F.B. de Bernard, M. Primet, H. Praliaud, Catal. Lett. 55 (1998) 217.
[28] J. Laine, F. Severino, Appl. Catal. 65 (1990) 253.
[29] P.W. Park, J.S. Ledford, Ind. Eng. Chem. Res. 37 (1998) 887.
[30] G. Xanthopoulou, G. Vekinis, Appl. Catal. B (1998) 37.
[31] A.L. Tarasov, M.O. Osmanov, V.A. Shvets, V.B. Kazanskii, Kinet. Catal. 31 (1990) 565.
[32] S. Stegenga, R. van Soest, F. Kapteijn, J.A. Moulijn, Appl. Catal. B 2 (1993) 257.
[33] F. Kapteijn, S. Stegenga, N.J.J. Dekker, J.W. Bijsterbosch, J.A. Moulijn, Catal. Today 16 (1993) 273.
[34] C.-Y. Lee, T.-H. Jung, B.-H. Ha, Appl. Catal. B 9 (1996) 77.
[35] F.C. Meunier, V. Zuzaniuk, J.P. Breen, M. Olsson, J.R.H. Ross, Catal. Today 59 (2000) 287.
[36] K.-I. Shimizu, J. Shibata, H. Yoshida, A. Satsuma, T. Hattori, Appl. Catal. B 30 (2001) 151.
[37] T. Furusawa, K. Seshan, J.A. Lercher, L. Lefferts, K.-I. Aika, Appl. Catal. B 37 (2002) 205.
[38] N.A.S. Amin, E.F. Tan, Z.A. Manan, Appl. Catal. B 43 (2003) 57.
[39] T.E. Hoost, R.J. Kudla, K.M. Collins, M.S. Chattha, Appl. Catal. B (1997) 59.
[40] J.R. Anderson, Structure of Metallic Catalysts, Academic Press, New York, 1975, p. 163.
[41] V.Z. Fridman, L.N. Bedina, I.Y. Petrov, Kinet. Catal. 29 (1988) 535.
[42] V.Z. Fridman, E.D. Mikhal'chenko, B.G. Tryasunov, A.V. Ziborov, L.M. Plyasova, Kinet. Catal. 32 (1991) 831.
[43] C.-C. Chien, W.-P. Chuang, T.-J. Huang, Appl. Catal. A 131 (1995) 73.
[44] L. Dong, Y. Hu, M. Shen, T. Jin, J. Wang, W. Ding, Y. Chen, Chem. Mater. 13 (2001) 4227.
[45] A. Jones, B. McNicol, Temperature Programmed Reduction for Solid Materials Characterization, Dekker, New York, 1986, p. 81.
[46] N. Aoyama, Y. Yamashita, A. Abe, N. Takezawa, K. Yoshida, Phys. Chem. Chem. Phys. 1 (1999) 3365.
[47] A. Martínez-Arias, M. Fernández-García, A. Iglesias-Juez, J.A. Anderson, J.C. Conesa, J. Soria, Appl. Catal. B 28 (2000) 29.
[48] D. Pietrogiacomi, S. Tuti, M.C. Campa, V. Indovina, Appl. Catal. B 28 (2000) 43.
[49] K.C.C. Kharas, Appl. Catal. B 2 (1993) 207.
[50] J.O. Petunchi, W.K. Hall, Appl. Catal. B 2 (1993) L17.
[51] J.A. Anderson, C. Márquez-Alvarez, M.J. López-Muñoz, I. Rodríguez-Ramos, A. Guerrero-Ruiz, Appl. Catal. B. 14 (1997) 189.
[52] E. Kikuchi, K. Yogo, Catal. Today 22 (1994) 73.
[53] K. Krantz, S. Ozturk, S. Senkan, Catal. Today 62 (2000) 281.
[54] R. Hernández-Huesca, J. Santamaría-González, P. Braos-García, P. Maireles-Torres, E. Rodríguez-Castellón, A. Jiménez-Lopéz, Appl. Catal. B 29 (2001) 1.
[55] M. Misono, C. Yokoyama, Catal. Today 22 (1994) 59.
[56] H. Hamada, Y. Kintaichi, M. Sasaki, T. Ito, M. Tabata, Appl. Catal. 70 (1991) L15.
[57] K. Yogo, M. Ihara, I. Terasaki, E. Kikuchi, Appl. Catal. B 2 (1993) L1.
[58] G.R. Bamwenda, A. Ogata, A. Obuchi, J. Oi, K. Mizuno, J. Skrzypek, Appl. Catal. B 6 (1995) 311.
[59] R. Burch, P.J. Millington, Appl. Catal. B 2 (1993) 101.
[60] S.E. Maisuls, K. Seshan, S. Feast, J.A. Lercher, Appl. Catal. B 29 (2001) 69.
[61] J.L. d'Itri, W.M.H. Sachtler, Appl. Catal. B 2 (1993) L7.
[62] H. Hamada, Y. Kintaichi, M. Sasaki, T. Ito, Chem. Lett. (1990) 1069.